






ORIGINAL RESEARCH

Larynx proteomics after jellyfish collagen IL: Increased ECM/collagen and suppressed inflammation

Andrew J. Bowen MD MS¹  | Dale C. Ekbom MD¹  | Danielle Hunter BSc¹ |
Stephen Voss MS¹  | Kathleen Bartemes PhD¹ | Andrew Mearns-Spragg PhD² |
Michael S. Oldenburg MD³  | Serban San-Marina PhD¹ 

¹Mayo Clinic ENT, Rochester, Minnesota, USA

²Jellagen Ltd., Wentloog Industrial Estate, Cardiff, UK

³Prevea Health Services, Green Bay, Wisconsin, USA

Correspondence

Serban San-Marina, Mayo Clinic ENT, 200 1st St SW, Rochester, MN, USA.

Email: ssanmarina@gmail.com

Funding information

Jellagen Ltd., Unit G6, Capital Business Park, Parkway Wentloog Industrial Estate, Cardiff, UK, CF3 3PY TEL +44(0)3333 583 299

Abstract

Objectives/Hypothesis: Compare proteomic profiles of rabbit vocal folds (VFs) injected with micronized cross-linked jellyfish collagen “collagen Type 0” (MX-JC) against two clinical products for injection medialization laryngoplasty (IL).

Study Design: Animal model.

Methods: Left recurrent laryngeal nerve sectioning and IL were performed in New Zealand White rabbits ($N = 6/\text{group}$). Group 1 received (MX-JC) and adipose-derived stem cells (ADSCs), Group 2, MX-JC alone; Group 3, cross-linked hyaluronic acid; and Group 4, micronized acellular dermis. Animals were sacrificed at 4 and 12 weeks. Proteomic profiling of injected versus noninjected VFs by nano-liquid chromatography, tandem mass spectrometry, and reactome gene ontology analysis was performed.

Results: Overall, 37–61 proteins were found to be upregulated and 60–284 downregulated in injected versus non-injected VFs (>1.5 fold, false discovery rate-adjusted $p < .05$). Over-representation analysis (% of total) revealed top up-regulated pathways at 4 and 12 weeks, respectively: Group 1, keratan sulfate metabolism (46%) and cellular processes (29%); Group 2, extracellular matrix (ECM)/collagen processes (33%) and beta oxidation (39%); Group 3, cellular processes (50%) and energy metabolism (100%); and Group 4, keratan sulfate metabolism (31%) and inflammation (50%). Top downregulated pathways were: Group 1, Inflammation (36%) and glucose/citric acid metabolism (42%); Group 2, cell signaling (38%) and glucose/citric acid metabolism (35%); Group 3, keratan sulfate metabolism (31%) and ECM/collagen processes (48%); and Group 4, glucose/citric acid metabolism (33%) and ECM/collagen processes (43%).

Conclusions: MX-JC “collagen Type 0” upregulates pathways related to ECM/collagen formation and downregulates pathways related to inflammation suggesting that it is promising biomaterial for IL.

Level of Evidence: NA

This is an open access article under the terms of the [Creative Commons Attribution-NonCommercial-NoDerivs](https://creativecommons.org/licenses/by-nc-nd/4.0/) License, which permits use and distribution in any medium, provided the original work is properly cited, the use is non-commercial and no modifications or adaptations are made.

© 2022 The Authors. *Laryngoscope Investigative Otolaryngology* published by Wiley Periodicals LLC on behalf of The Triological Society.

KEYWORDS

collagen type 0, Cymetra[®], hyaluronic acid, injection laryngoplasty, Jellagen[®], jellyfish collagen, micronized acellular dermis, plasmocytic immunity, Restylane[®], stem cells, T-cell response

1 | INTRODUCTION

Unilateral vocal fold paralysis (UVFP) has an estimated incidence of 1–5 per 100,000 in the general population^{1,2} and a multifactorial etiology, with thyroid and nonthyroid surgery as primary drivers, followed by malignancy and idiopathic causes.³ Injection medialization laryngoplasty (IL) is a temporary, first-line treatment for UVFP, that aims to correct voice communication and restore glottal competence. IL delivers volume-augmenting materials close to the paralyzed VF thus aiming to bring it to the midline. The procedure has a 110-year history, dating back to Bruening's pioneering work with paraffin.⁴ Successes, as well as failures with various protocols and biomaterials, have been amply described.^{5,6} Most biomaterials aim to achieve an optimal balance between ease of injection, duration of laryngeal closure, and degree of restored phonation. Current outpatient interest revolves around compounds that can be delivered with smaller bore needles under local anesthesia, are well tolerated, and do not migrate.⁷ Although many of the studies described in the literature have generated useful data on some aspects of the laryngeal parenchymal response to biomaterials, there is a need for benchmarking these responses at the molecular level. This endeavor may help guide the design of future, more personalized IL approaches.

Collagen is essential for extracellular matrix (ECM) formation and is widely used in tissue engineering applications.⁸ Jellagen[®] marine collagen is a nonmammalian "Collagen Type 0" extracted from the "barrel jellyfish" (*Rhizostoma pulmo*) that grows abundantly off the coast of Western Wales, UK where it is harvested and processed for medical and research applications. Well-regulated ISO13485:2016 protocols ensure batch-to-batch consistency⁹ and thus experimental reproducibility. This archaic "Collagen Type 0" is phylogenetically related to mammalian collagen I, II, III, V, and IX and shares many functions across these specialized collagens. In animal models, Jellagen[®] "Collagen Type 0" had lower immunogenicity compared with mammalian collagens and generated a >40% increase in de novo tissue (bone) formation.¹⁰

Our prior IL work with this material, as a micronized, cross-linked collagen Jellagen[®] injectable (MX-JC, Jellagen[®]) in rabbits with recurrent laryngeal nerve (RLN) transection demonstrated lower resorption rates and a lower-grade inflammatory response, compared with cross-linked hyaluronic acid (X-HA, Restylane[®]) and human micronized acellular cadaveric dermis (MACD, Cymetra[®]), two biomaterials that are widely used in the clinic.¹¹ Here, we analyze the molecular responses of the laryngeal parenchyma to these biomaterials in order to identify pathways and mechanisms that account for the beneficial IL properties of MX-JC, relative to MACD and X-HA. To this end, we performed proteomic analyses of formalin-fixed, paraffin-embedded (FFPE) laryngeal tissue sections

at 4 and 12 weeks after IL, using nanoflow liquid chromatography electrospray ionization tandem mass spectrometry (nLC-MS/MS), followed by Reactome Gene Ontology pathway analysis.^{12,13} We find that MX-JC upregulates extracellular basement membrane (ECM)/collagen-related processes and downregulates inflammation pathways, whereas MACD does the reverse. Furthermore, while MX-JC switches energy production to beta oxidation that is known to promote myoblast-dependent tissue remodeling/regeneration,^{8,14} MACD downregulates these processes, which promotes scarring.¹⁵ These promising results indicate that MX-JC in addition to IL tissue augmentation may have unique regenerative and anti-inflammatory properties compared with MACD and X-HA, that could benefit its clinical IL application.

2 | METHODS

2.1 | Animals

All experiments were performed according to the Guide for the Care and Use of Laboratory Animals and the US Public Health Service's Policy on Humane Care and Use of Laboratory Animals. All research protocols were performed after thorough review and approval from Mayo Clinic Institutional Animal Care and Use Committee (IACUC-no. A4201). Whole tissue proteome analysis was performed on 11 rabbit larynges, comparing injected to contralateral, uninjected VFs, at 4 and 12 weeks post-IL. For each group, three injected animals were available per time point, except for the 4-week MACD group which had only two animals.

2.2 | Sample preparation

Our rabbit model for IL was previously described.¹¹ Briefly, following left RLN transection, IL was performed by Mayo ENT surgical staff via a free hand procedure using 100 μ l of MX-JC, MX-JC + ADSCs, MACD, or X-HA. Animals were sacrificed 4 or 12 weeks later, and larynges were preserved as FFPE tissue blocks for processing. Each block was subdivided into three sub-blocks of relatively equal size and single, 5- μ m thick axial cross-section slices from each sub-block, were colayered on histology slides so that all blocks were represented on the same slide. A total of 25 slides (75 tissue sections from 3 blocks) per animal were available for further processing. After staining with hematoxylin and eosin and photography for digital record keeping, tissue collection for mass spectrometry analysis was performed as before.¹⁶ Briefly, ellipsoid-shaped sections from the injected (test or T) and uninjected, contralateral (control, or C), tissue were scraped off the FFPE slides with disposable scalpels, weighed, and pooled into 1.5-ml polypropylene microfuge tubes, for protein

analysis by nLC-MS/MS, at the Medical Genome Facility-Proteomics of the Mayo Clinic, Rochester, Minnesota.

2.3 | Peptide identification by nLC-MS/MS analysis

The detailed protocol for nLC-MS/MS analysis was previously reported.¹⁶ Briefly, solubilization of collected tissue was performed in 2% sodium dodecyl sulfate (SDS)/50 mM Tris (pH 8.2), followed by reduction with 10 mM Tris-(carboxyethyl) phosphine hydrochloride and cysteine alkylation with 10-mM iodoacetamide. After SDS removal samples were digested with 1:50 trypsin solution and peptides were separated by nano-liquid chromatography (nLC) using a Q-Exactive mass spectrometer coupled to a Dionex 3000 Rapid Separation Liquid Chromatography nano liquid chromatograph (Thermo Fisher Scientific, Bremen, Germany), with a mixture of solvents containing water, formic acid, acetonitrile, and iso-propanol at a rate of 400 nl/min using PicoFrit/Agilent Poroshell-packed columns. Mass spectrometry data were acquired throughout the LC gradient using a data dependent acquisition method that repetitively acquired MS1 spectra (m/z 340–1600) of the intact peptides at 70,000 resolving power (RP = 70,000, FWHM at m/z 200, automatic gain control [AGC] = $3e6$, max fill time of 150 ms), followed by acquiring MS2 spectra for the top 20 abundant peptides (RP = 17,500, AGC = $1e5$, isow = 2.5, NCE = 27, max fill time of 70 ms). Precursors selected for an MS2 experiment were excluded from re-selection for 30s.

2.4 | Database searching and criteria for protein identification

MaxQuant (ver. 1.6.7.0) was used to search raw data files for peptide sequence and protein assignment and to record protein relative intensities for each sample. MS2 spectra were searched against a composite fasta file of Uniprot entries (release 2020–03, downloaded July 17, 2020). SwissProt and TRMBL entries were used for rabbit (OX = 9986). Perseus (ver. 1.6.7.0) was used to perform *t*-tests between groups on Log2 transformed data and plot protein concentration trend lines across the samples.

2.5 | Proteomics data processing

Further data analysis was performed using Orange software (<https://orangedatamining.com>). Missing values were removed, proteins with at least two unique peptides were selected, and group normalization by standardization (mean = 0, SD = 1) followed by K means clustering analysis were performed to identify patterns of expression similarity. After Bonferroni correction for multiple comparisons, up and downregulated proteins with 1.5-fold or greater expression and *p* values < .05, were segmented by sample and protein type. The lists of up- and downregulated proteins that satisfied these criteria and

were present in all animals belonging to a specific group and time point are shown as Supporting Information S1.

2.6 | Reactome enrichment analysis

Using the protein lists, upregulated and downregulated pathways were identified with Reactome software (version 74)^{12,13} for pathway over-representation. After correction for false discovery rate,³ lists of the top 25 most significant up and downregulated pathways for each time point and group were generated (Supporting Information S2). Because up and downregulated proteins can belong to the same pathway, a disambiguation process was performed to analyze pathways that contain either upregulated proteins or downregulated proteins.¹⁷ The disambiguation process consisted of removing from the pathway analyses pathways that contained both up- and downregulated proteins, so that only pathways that contained either all up-regulated or all downregulated proteins, but not both, were considered.

2.7 | Delta score evaluation of responses

In order to evaluate the relative contribution of ontologies ECM/collagen metabolism, inflammation, motility, proteoglycan metabolism, and energy utilization to the overall tissue response to the tested biomaterials, we calculated a delta score by subtracting the number of downregulated pathways from the number of upregulated pathways. A positive score suggests the preponderance of upregulatory drivers while a negative score suggests the reverse.

3 | RESULTS

3.1 | Proteomics

Up- and downregulated proteins with 1.5-fold or better enrichment ($p < .05$ after Bonferroni correction) in injected relative to uninjected, contralateral, VFs are shown in Figure 1A and Supporting Information S1. The number of statistically significantly enriched Reactome pathways constructed from these proteins ($p < .05$ after correction for false discovery rate) are shown in Figure 1B. Distribution of the top 25 most significant pathways is shown in Figure 1C and Supporting Information S2. Overall, ~40% of the top 25 pathways were upregulated, 40% downregulated, and 20% contained both up- and downregulated proteins.

3.2 | Reactome pathway analysis

To summarize the data, we focused on the top 25 Reactome pathways that were up- or downregulated in injected relative to uninjected VFs (Figure 1C). From each group, we identified ontologies that accounted for >50% of the data and allowed comparisons across groups, namely: (1) ECM/collagen metabolism, (2) inflammation, (3) motility,

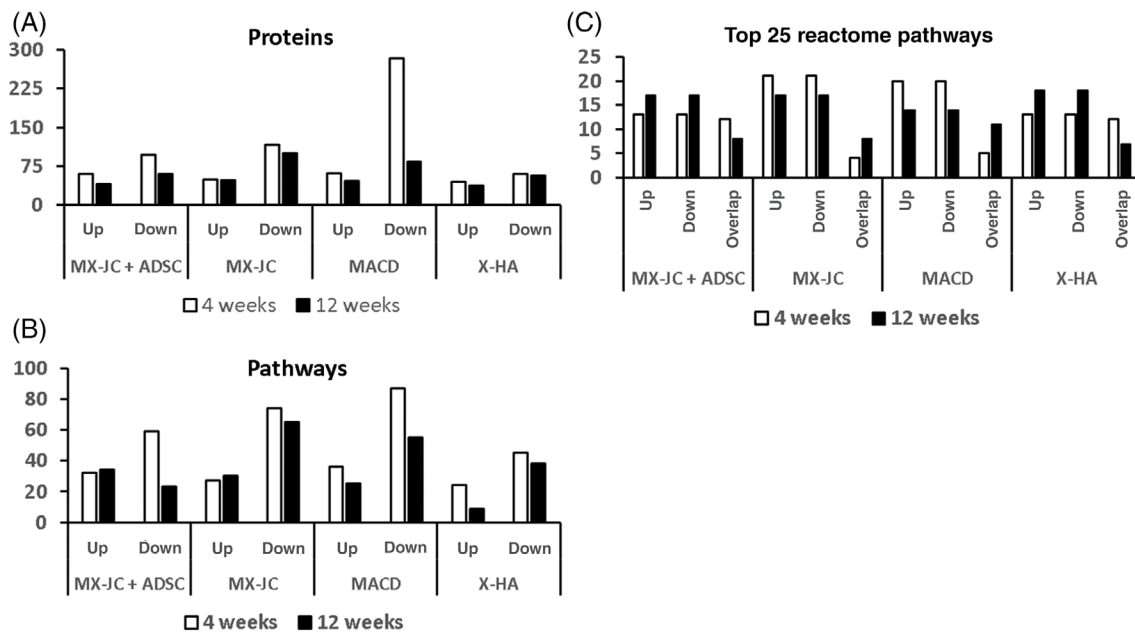


FIGURE 1 nLC-MS/MS changes in rabbit VF proteome after IL. (A) Up- and downregulated proteins at 4 and 12 weeks. Data show the number of proteins in injected versus noninjected VFs (1.5-fold or greater change, $p < .05$ after Bonferroni correction), that were common for all animals in the respective groups. (B) Number of Reactome pathways that implicate the proteins in (A). Data show pathways with $p < .05$ enrichment score after Bonferroni correction and include overlapping pathways. (C) Top 25 Reactome pathways segregated by up-/downregulated and overlapping pathways. IL, tissue collection and data analysis, and pathway analysis using Reactome software^{12,13} are described in Section 2. For simplification, data show only proteins and pathways that were common to all animals for each respective group and time point. Abbreviations: ADSC, adipose-derived stem cell; IL, Injection medialization laryngoplasty; MACD, micronized acellular dermis; MX-JC, micronized cross-linked jellyfish collagen; nLCMS/MS, nanoflow liquid chromatography electrospray ionization tandem mass spectrometry; VF, vocal fold; X-HA, cross-linked hyaluronic acid.

TABLE 1 Principal up- and downregulated cellular processes in the VF proteome after IL

Group	4 weeks				12 weeks			
	Up	%	Down	%	Up	%	Down	%
MX-JC + ADSC	Keratan sulfate metabolism	46	Inflammation	36	Cellular processes	29	Glucose/citric acid metabolism	42
	Glucose metabolism	27	Citric acid cycle	27	Muscle contraction	24	Mitochondria regulation	17
	Others	27	Others	37	Others	47	Others	41
MX-JC	ECM/collagen processes	34	Cell signaling	38	Beta oxidation for energy metabolism	39	Glucose/citric acid metabolism	35
	Cell motility	33	Inflammation	33	Injury response	15	Inflammation	30
	Others	33	Others	29	Others	46	Others	35
MACD	Keratan sulfate metabolism	31	Glucose/citric acid metabolism	33	Inflammation	50	ECM/collagen processes	43
	Glucose metabolism	25	T1 Inflammation	18	Proteoglycan metabolism	30	Cell motility	21
	Others	44	Others	49	Others	20	Others	36
X-HA	Cellular processes	50	Keratan sulfate metabolism	31	Energy metabolism	100	ECM/collagen processes	48
	Mitochondria regulation	25	Glucose metabolism	23			Cell motility	14
	Others	25	Others	46			Others	38

Abbreviations: ADSC, adipose-derived stem cell; ECM, extracellular matrix; IL, Injection medialization laryngoplasty; MACD, micronized acellular dermis; MX-JC, micronized cross-linked jellyfish collagen; VF, vocal fold; X-HA, cross-linked hyaluronic acid.

(4) proteoglycan metabolism, and (5) energy utilization (glucose, citric acid, and mitochondria metabolism, energy regulation; Table 1). ECM/collagen metabolism was upregulated in MX-JC and downregulated in MACD and X-HA. Similarly, in the MX-JC group, downregulation of inflammation accounted for 33% and 30% of pathways at 4 and 12 weeks post-IL, respectively (Table 1). In the MACD group, downregulation of inflammation accounted for only 17% of pathways at 4 weeks, while at 12 weeks

post-IL 50% of upregulated pathways related to inflammation (Table 1). Furthermore, while in MX-JC cellular motility was upregulated, both MACD and X-HA showed the opposite effect, albeit at different time points (Table 1). Interestingly, proteoglycan and specifically keratan sulfate metabolism were also differentially regulated in three of the groups. It increased in MX-JC + ADSC and MACD groups but decreased in X-HA (Table 1). Notably, with respect to energy utilization in the MX-JC group,

TABLE 2 Net direction of the regulation of cellular processes

Pathways	MX-JC		MX-JC + ADSC		MACD		X-HA	
	4 weeks	12 weeks	4 weeks	12 weeks	4 weeks	12 weeks	4 weeks	12 weeks
ΔECM/collagen	1	1	1	0	0	-5	0	-8
ΔEnergy	-2	-1	0	-2	0	-2	0	5
ΔInflammation	-6	-5	-4	0	-2	5	0	5
ΔMotility	3	-1	0	3	-3	-3	1	-3
ΔProteoglycans	0	0	6	0	9	2	-6	-4

Note: Data shown were calculated by summing up the number of up- and downregulated pathways associated with respective cellular processes.

Abbreviations: ADSC, adipose-derived stem cell; ECM, extracellular matrix; MACD, micronized acellular dermis; MX-JC, micronized cross-linked jellyfish collagen; X-HA, cross-linked hyaluronic acid.

TABLE 3 Biomaterial-specific pathways

Group	Pathways	Description	Time	Direction	Reactome ID
MX-JC	ECM/collagen	Nonintegrin membrane-ECM interactions	4	↑	R-HSA-2243919
	Energy	Crosslinking of collagen fibrils	4	↑	R-HSA-1430728
		Mitochondrial fatty acid beta-oxidation of saturated fatty acids	12	↑	R-HSA-77286
		Beta oxidation of palmitoyl-CoA to myristoyl-CoA	12	↑	R-HSA-77305
	Inflammation	Beta oxidation of lauroyl-CoA to decanoyl-CoA-CoA	12	↑	R-HSA-77310
		Immune system	4	↓	R-HSA-168256
Innate immune system		12	↓	R-HSA-168249	
MX-JC + ADSC	ECM/collagen	Regulation of IGF transport and uptake by IGFs	12	↑	R-HSA-381426
	Energy	Mitochondrial biogenesis	12	↓	R-HSA-1592230
		Metabolism	12	↓	R-HSA-611105
	Inflammation	Platelet degranulation	12	↓	R-HSA-114608
MACD	Energy	Translocation of SLC2A4 (GLUT4) to the plasma membrane	4	↓	R-HSA-1445148
	Inflammation	HSF1 activation	4	↑	R-HSA-3371511
		Cytokine Signaling in Immune system	12	↑	R-HSA-1280215
		Signaling by Interleukins	12	↑	R-HSA-449147
	Proteoglycan	Diseases of glycosylation	4	↑	R-HSA-3781865
		Defective B3GAT3 causes JDSSDHD	12	↑	R-HSA-3560801
		Defective B3GALT6 causes EDSP2 and SEMDJL1	12	↑	R-HSA-4420332
X-HA	ECM/collagen	Degradation of the extracellular matrix	12	↓	R-HSA-1474228
		Collagen biosynthesis and modifying enzymes	12	↓	R-HSA-1650814
		Nonintegrin membrane-ECM interactions	12	↓	R-HSA-3000171
		Collagen chain trimerization	12	↓	R-HSA-8948216
	Energy	Transcriptional activation of mitochondrial biogenesis	4	↑	R-HSA-2151201

Abbreviations: ADSC, adipose-derived stem cell; ECM, extracellular matrix; IGF, insulin-like growth factor; IGFs, IGF binding proteins; MACD, micronized acellular dermis; MX-JC, micronized cross-linked jellyfish collagen; X-HA, cross-linked hyaluronic acid.

there was a switch to fatty acid beta oxidation metabolism at 12 weeks, a pathway (R-HSA-77286) associated with new muscle fiber formation.¹⁸

3.3 | Delta score evaluation of responses

Delta scores depicting the contribution of each of the five ontologies to the tissue response for each of the biomaterials are shown in Table 2. Positive values indicate a preponderance of positive regulatory drivers and negative values indicate the opposite. The largest score change was in proteoglycan metabolism (+9, MACD 4 weeks), followed by ECM/collagen (−8, X-HA, 12 weeks), and inflammation (−6, MX-JC 4 weeks).

3.4 | Biomaterial-specific reactome pathways

Next, we identified biomaterial-specific pathways for each experimental condition (Table 3). MX-JC and MACD led the count, with 7 unique pathways each, respectively ↑5 and ↓2 and ↑6 and ↓1, followed by X-HA with 5 (↑1, and ↓4), and MX-JC + ADSC with 4 (↑1, and ↓3). In keeping with the delta scores, specific MX-JC pathways were associated with downregulation of inflammation and upregulation of fatty acid beta oxidation. Similarly, specific MACD pathways were associated with increased inflammation and proteoglycan-related disease pathways. The major effect of X-HA was to promote processes associated with ECM/collagen disruption.

4 | DISCUSSION

We previously reported on a novel jellyfish “Collagen Type 0” biomaterial for IL that outlasted Cymetra and Restylane, while producing minimal inflammation.¹ The current study investigates the molecular responses to these biomaterials using nLC-MS/MS analysis of FFPE tissue and Reactome proteomics. We find that (1) MX-JC is primarily associated with pathways related to upregulation of ECM/collagen, downregulation of inflammation, a switch to energy production through beta acid oxidation and increased proteoglycan synthesis, (2) MACD has biphasic effects on pathways related to inflammation, inhibitory at 4 weeks and proinflammatory at 12 while X-HA upregulates pro-inflammatory pathways (Table 1), and (3) MACD and X-HA have opposing regulatory effects on pathways related to proteoglycan metabolism (Table 1).

As part of the Harmonizome project, 75 highly expressed housekeeping proteins were identified in the larynx.¹⁹ Interestingly, only 2.9% and 2.2% of the up- and downregulated proteins, respectively, from this study are represented in this panel. This suggests the presence of a subset of biomaterials-inducible proteins that are separate from the housekeeping laryngeal proteins in the Harmonizome study.

Global changes in the laryngeal proteome in response to external factors have not been studied at length. Only a handful of studies have addressed changes in the laryngeal proteome as they relate to

cigarette smoke exposure,²⁰ senescent muscle,²¹ systemic dehydration,²² decellularization,²³ and cancer.^{24–29} However, in a literature search on laryngeal proteomics following IL, the only entries were two previous studies from our group.^{16,30}

4.1 | ECM/collagen metabolism

The importance of collagen biosynthesis to the integrity of the ECM is well established.^{8,31} Studying bioactive protein remnants in a decellularized human VF mucosa model, Welham et al.²³ report abundant levels of collagen α-3(VI) chain, collagen α-2(VI) chain, collagen α-1(VI) chain, collagen α-1(VII) chain, and collagen alpha-2(I) chain. We found that post-IL, ECM/collagen processes are upregulated in MX-JC (4 weeks) and downregulated in MACD and X-HA groups (12 weeks), indicating a potential ECM benefit for MX-JC over MACD (Table 1). Furthermore, downregulation of collagen biosynthesis may impact capillary integrity, as Gugatschka et al.,²⁰ report that pronounced histological changes such as damaged microvessels or immune cell infiltration of the VF connective tissue are associated with impaired fibrillary collagen (Col1A1, Col1A2, and Col3A1) and hyaluronan biosynthesis.

4.2 | Inflammation

Downregulation of pathways related to inflammation in the MX-JC group accounted for 33% and 30% of all pathways at 4 and 12 weeks, respectively (Table 1), with specific downregulation of T1 inflammation pathways R-HSA-168256 and R-HSA-168249 (Table 3). In contrast, MACD showed a biphasic effect on inflammation-related pathways with modest downregulation at 4 weeks and pronounced upregulation at 12 weeks (Table 1). Three specific inflammatory pathways were upregulated: R-HSA-3371511, R-HSA-1280215, and R-HSA-449147 (Table 3). These findings suggest that jellyfish and cadaveric dermis-derived materials, trigger opposite inflammatory responses in the native laryngeal parenchyma. T1 inflammation is a cell-mediated immune response characterized by activation of macrophages and cytotoxic T-cells by tumor necrosis factor-alpha and interferon-gamma.³² In keeping with our findings, downregulation of T1 inflammation by jellyfish “Collagen Type 0” was previously reported.^{10,33,34} Generic upregulation of inflammation observed with MACD may have a volume-filling effect; in the presence of an inflammatory infiltrate there is an initial medialization benefit followed by scar formation. In keeping with the current findings, we previously demonstrated lymphocytic infiltration at the MACD injection site.¹¹ In contrast, MX-JC appears to exert its volumetric IL benefit primarily by promoting ECM/collagen biosynthesis.

4.3 | Proteoglycans and metabolism

Keratan and generic proteoglycan metabolism accounted for 30% and 46% of upregulated pathways in MX-JC + ADSC and MACD,

respectively, and 31% of downregulated pathways in X-HA (Table 1). For MACD, one specific pathway (R-HSA-3781865) was upregulated at 4 weeks and two others at 12 weeks (R-HSA-3560801 and R-HSA-4420332; Table 3). Within the ECM of the vocal cord keratan sulfate is abundant within the deep lamina propria where it forms fibromodulin, a proteoglycan responsible for organizing collagen fibrils within the deepest most dense portions of the vocal ligament.^{31,35,36} The upregulation of glycoprotein pathways could represent ongoing extracellular remodeling processes as previously reported.¹⁴ These processes likely occur within myofibroblasts which are responsible for maintenance and repair of the ECM postinjury.^{37,38}

4.4 | Metabolic processes

Energy metabolism regulation varied across groups and time points. Beta-oxidation of fatty acids increased at 12 weeks in MX-JC and MX-JC + ADSC (Table 1). This is known to promote formation of new muscle fibers^{39,40} and may be seen in the larger context of pro-regenerative signals associated to “collagen type 0.” Three specific fatty acid beta oxidation pathways were upregulated in MX-JC at 12 weeks post-IL: R-HSA-77286, R-HSA-77305, and R-HSA-77310 (Table 2). Since inhibition of fatty acid oxidation was shown to promote fibrotic skin tissue¹⁵ upregulation of fatty acid oxidation may decrease scar formation, although the extent to which these findings with dermal fibroblasts can be extrapolated to the larynx remains to be determined.

4.5 | Limitations

We acknowledge several limitations in our study. First, because we focus on proteomic ontologies that account for >50% of data we leave out an analysis of lesser ontologies and other pathways that may play important roles in the observed responses. Furthermore, for all groups, pathways tagged by both up- and downregulated proteins were excluded from analysis, yet these pathways may contain important information related to the overall response of the laryngeal parenchyma to the biomaterials used in this study.

5 | CONCLUSION

We identify major proteomic changes post-IL in ECM/Collagen metabolism, inflammation, energy, motility, and proteoglycan metabolism, triggered by the IL biomaterials. MX-JC “Collagen Type 0” has unique features as it suppresses pathways related to inflammation, including T1 inflammation, promotes pathways related to ECM/collagen synthesis, suggesting tissue restorative properties, as well as promoting energy production through beta acid oxidation, presumably by targeting myofibroblast populations and potentially triggering proregenerative responses. These results are encouraging with respect to the potential use of “Collagen Type 0” as an alternative IL material in the clinic or operating room enabling better tissue augmentation and restorative outcomes.

FUNDING INFORMATION

Funds for the project were provided in part by Jellagen Pty Ltd. under a work agreement with the Mayo Clinic, with Serban San-Marina and Dale C. Ekbom as Principal IACUC Investigators.

CONFLICT OF INTEREST

The study authors declare no competing financial interests. Serban San-Marina is a member of the Scientific Advisory Board for Jellagen Ltd.

ORCID

Andrew J. Bowen  <https://orcid.org/0000-0002-6542-7932>

Dale C. Ekbom  <https://orcid.org/0000-0001-8770-8463>

Stephen Voss  <https://orcid.org/0000-0001-8010-961X>

Michael S. Oldenburg  <https://orcid.org/0000-0002-5419-7748>

Serban San-Marina  <https://orcid.org/0000-0002-5312-4774>

REFERENCES

1. Korean Society of Laryngology, Phoniatics, Logopedics Guideline Task Force et al. Guidelines for the management of unilateral vocal fold paralysis from the Korean Society of Laryngology, Phoniatics and Logopedics. *Clin Exp Otorhinolaryngol*. 2020;13:340-360.
2. Masroor F, Pan DR, Wei JC, Ritterman Weintraub ML, Jiang N. The incidence and recovery rate of idiopathic vocal fold paralysis: a population-based study. *Eur Arch Otorhinolaryngol*. 2019;276:153-158.
3. Spataro EA, Grindler DJ, Paniello RC. Etiology and time to presentation of unilateral vocal fold paralysis. *Otolaryngol Head Neck Surg*. 2014;151:286-293.
4. Brunings W. Über eine neue Behandlungsmethode der Rekurrenslähmung. *Verh Dtsch Laryngol*. 1911;18:93-98.
5. Li L, Stiadle JM, Lau HK, et al. Tissue engineering-based therapeutic strategies for vocal fold repair and regeneration. *Biomaterials*. 2016;108:91-110.
6. Mallur PS, Rosen CA. Vocal fold injection: review of indications, techniques, and materials for augmentation. *Clin Exp Otorhinolaryngol*. 2010;3:177-182.
7. Eppley BL, Dadvand B. Injectable soft-tissue fillers: clinical overview. *Plast Reconstr Surg*. 2006;118:98e-106e.
8. Bielajew BJ, Hu JC, Athanasiou KA. Collagen: quantification, biomechanics, and role of minor subtypes in cartilage. *Nat Rev Mater*. 2020;5:730-747.
9. Widdowson JP, Picton AJ, Vince V, Wright CJ, Mearns-Spragg A. In vivo comparison of jellyfish and bovine collagen sponges as prototype medical devices. *J Biomed Mater Res B Appl Biomater*. 2018;106:1524-1533.
10. Flaig I, Radenkovic M, Najman S, Prohl A, Jung O, Barbeck M. In vivo analysis of the biocompatibility and immune response of jellyfish collagen scaffolds and its suitability for bone regeneration. *Int J Mol Sci*. 2020;21:4518.
11. San-Marina S, Bowen AJ, Oldenburg MS, et al. MRI study of jellyfish collagen, hyaluronic acid, and cadaveric dermis for injection Laryngoplasty. *Laryngoscope*. 2021;131:E2452-E2460.
12. Fabregat A, Korninger F, Viteri G, et al. Reactome graph database: efficient access to complex pathway data. *PLoS Comput Biol*. 2018;14:e1005968.
13. Jassal B, Matthews L, Viteri G, et al. The reactome pathway knowledgebase. *Nucleic Acids Res*. 2020;48:D498-D503.
14. Nakamura R, Doyle C, Bing R, Johnson AM, Branski RC. Preliminary investigation of in vitro, bidirectional vocal fold muscle-mucosa interactions. *Ann Otol Rhinol Laryngol*. 2022;131(5):512-519.

15. Zhao X, Psarinos P, Ghorai LS, et al. Metabolic regulation of dermal fibroblasts contributes to skin extracellular matrix homeostasis and fibrosis. *Nat Metab.* 2019;1:147-157.
16. Voss S, San-Marina S, Oldenburg MS, et al. Histone variants as stem cell biomarkers for long-term injection medialization Laryngoplasty. *Laryngoscope.* 2018;128:E402-E408.
17. Hong G, Zhang W, Li H, Shen X, Guo Z. Separate enrichment analysis of pathways for up- and downregulated genes. *J R Soc Interface.* 2014;11(92):20130950.
18. Henique C, Mansouri A, Vavrova E, et al. Increasing mitochondrial muscle fatty acid oxidation induces skeletal muscle remodeling toward an oxidative phenotype. *FASEB J.* 2015;29:2473-2483.
19. Santos A, Tsafou K, Stolte C, Pletscher-Frankild S, O'Donoghue SI, Jensen LJ. Comprehensive comparison of large-scale tissue expression datasets. *PeerJ.* 2015;3:e1054.
20. Gugatschka M, Darnhofer B, Grossmann T, et al. Proteomic analysis of vocal fold fibroblasts exposed to cigarette smoke extract: exploring the pathophysiology of Reinke's edema. *Mol Cell Proteomics.* 2019;18:1511-1525.
21. Shembel AC, Kanshin E, Ueberheide B, Johnson AM. Proteomic characterization of senescent laryngeal adductor and Plantaris Hindlimb muscles. *Laryngoscope.* 2022;132:148-155.
22. do Nascimento NC, Dos Santos AP, Mohallem R, et al. Furosemide-induced systemic dehydration alters the proteome of rabbit vocal folds. *J Proteomics.* 2022;252:104431.
23. Welham NV, Chang Z, Smith LM, Frey BL. Proteomic analysis of a decellularized human vocal fold mucosa scaffold using 2D electrophoresis and high-resolution mass spectrometry. *Biomaterials.* 2013;34:669-676.
24. Sewell DA, Yuan CX, Robertson E. Proteomic signatures in laryngeal squamous cell carcinoma. *ORL J Otorhinolaryngol Relat Spec.* 2007;69:77-84.
25. Weinberger PM, Merkley M, Lee JR, et al. Use of combination proteomic analysis to demonstrate molecular similarity of head and neck squamous cell carcinoma arising from different subsites. *Arch Otolaryngol Head Neck Surg.* 2009;135:694-703.
26. Li L, Zhang Z, Wang C, et al. Quantitative proteomics approach to screening of potential diagnostic and therapeutic targets for laryngeal carcinoma. *PLoS One.* 2014;9:e90181.
27. Liu J, Ma T, Gao M, et al. Proteomic characterization of proliferation inhibition of well-differentiated laryngeal squamous cell carcinoma cells under below-background radiation in a deep underground environment. *Front Public Health.* 2020;8:584964.
28. Liu J, Zhu W, Li Z, et al. Proteomic analysis of hypopharyngeal and laryngeal squamous cell carcinoma sheds light on differences in survival. *Sci Rep.* 2020;10:19459.
29. Liu H, Cui J, Zhang Y, et al. Mass spectrometry-based proteomic analysis of FSCN1-interacting proteins in laryngeal squamous cell carcinoma cells. *IUBMB Life.* 2019;71:1771-1784.
30. Janus JR, Voss SG, Madden BJ, et al. Time-course mass spectrometry data of adipose mesenchymal stem cells acquiring chondrogenic phenotype. *BMC Res Notes.* 2018;11:666.
31. Tang SS, Mohad V, Gowda M, Thibeault SL. Insights into the role of collagen in vocal fold health and disease. *J Voice.* 2017;31:520-527.
32. Mantovani A, Sica A, Sozzani S, Allavena P, Vecchi A, Locati M. The chemokine system in diverse forms of macrophage activation and polarization. *Trends Immunol.* 2004;25:677-686.
33. Morishige H, Sugahara T, Nishimoto S, et al. Immunostimulatory effects of collagen from jellyfish in vivo. *Cytotechnology.* 2011;63:481-492.
34. Song E, Yeon Kim S, Chun T, Byun HJ, Lee YM. Collagen scaffolds derived from a marine source and their biocompatibility. *Biomaterials.* 2006;27:2951-2961.
35. Hahn MS, Jao CY, Faquin W, Grande-Allen KJ. Glycosaminoglycan composition of the vocal fold lamina propria in relation to function. *Ann Otol Rhinol Laryngol.* 2008;117:371-381.
36. Pawlak AS, Hammond T, Hammond E, Gray SD. Immunocytochemical study of proteoglycans in vocal folds. *Ann Otol Rhinol Laryngol.* 1996;105:6-11.
37. Branco A, Bartley SM, King SN, Jette ME, Thibeault SL. Vocal fold myofibroblast profile of scarring. *Laryngoscope.* 2016;126:E110-E117.
38. Kumai Y. Pathophysiology of fibrosis in the vocal fold: current research, future treatment strategies, and obstacles to restoring vocal fold pliability. *Int J Mol Sci.* 2019;20(1):2551.
39. Fritzen AM, Lundsgaard AM, Kiens B. Tuning fatty acid oxidation in skeletal muscle with dietary fat and exercise. *Nat Rev Endocrinol.* 2020;16:683-696.
40. Houten SM, Wanders RJ. A general introduction to the biochemistry of mitochondrial fatty acid beta-oxidation. *J Inherit Metab Dis.* 2010;33:469-477.

SUPPORTING INFORMATION

Additional supporting information can be found online in the Supporting Information section at the end of this article.

How to cite this article: Bowen AJ, Ekblom DC, Hunter D, et al. Larynx proteomics after jellyfish collagen IL: Increased ECM/collagen and suppressed inflammation. *Laryngoscope Investigative Otolaryngology.* 2022;7(5):1513-1520. doi:10.1002/lio2.924